A Thermoelectric Battery Model for Post-Flood Geomagnetic Field Recovery: Quantitative Feasibility Analysis and Percolation-Threshold Dynamics

Peter Streitenberger, M.A.

Abstract

Background: Young-Earth chronological frameworks require geomagnetic field evolution on timescales of ≤4,000 years, with radiocarbon data suggesting a discrete transition (t_1) from weak to effective magnetic shielding within centuries of the Genesis Flood (2463 BC). Standard dynamo models, which operate on timescales of 10^5–10^6 years for thermal-convective coupling, cannot accommodate these constraints.

Objective: We construct and evaluate a thermoelectric (Seebeck-type) battery mechanism operating across the core–mantle boundary (CMB) as an alternative field source, focusing on: (1) whether such a mechanism can generate field strengths of observed magnitude, and (2) what physical processes could produce a sharp suppression → recovery transition on century-scale timescales.

Methods: We apply order-of-magnitude analysis using experimentally constrained parameters for Seebeck coefficients (10–300 μV/K for metal-silicate systems), electrical conductivities (10^2–10^6 S/m across the CMB region), and temperature gradients (2.5–10 K/km). We model the post-Flood CMB as a two-phase system (metallic FeSi particles dispersed in silicate matrix) and analyze electrical topology changes using percolation theory.

Results:

1. *Field magnitude:* A thermoelectric EMF of ~50 mV across the D″ layer can drive currents of ~10^9 A, generating dipole moments of ~10^{23} A·m² — comparable to or exceeding the observed terrestrial value (8×10^{22} A·m²). Field strength is not a limiting factor.
2. *Suppression mechanism:* Dispersion of metallic FeSi particles above the percolation threshold ($\varphi > \varphi_c \approx 0.16$–$0.29$) creates a low-resistance short-circuit path that bypasses the global current loop, suppressing effective field generation.
3. *Recovery mechanism:* Microstructural evolution — primarily Ostwald ripening at CMB temperatures (~4000 K) — reduces particle number density while increasing particle size, driving the system below the percolation threshold. This triggers an abrupt topological phase transition: the short-circuit network collapses, and the full thermoelectric EMF becomes available for global current flow.
4. *Transition sharpness:* The percolation transition exhibits critical behavior ($\sigma \propto [\varphi - \varphi_c]^t$ with $t \approx 2$), producing a sharp rather than gradual conductivity change. This naturally explains the discrete character of the t_1 transition inferred from radiocarbon data.
5. *Timescales:* Ostwald ripening rates extrapolated to CMB conditions ($K \sim 10^6$–10^9 μm³/yr) are consistent with percolation-threshold crossing within 10^2–10^3 years, though this extrapolation carries significant uncertainty.

Key Finding: The transition at t_1 is best understood as a percolation-threshold crossing — a topological phase transition — rather than as a gradual parametric change. The sharpness of the geomagnetic recovery and the coincident reduction in ^{14}C production rate are natural consequences of critical percolation dynamics.

Testable Predictions:

- Ostwald ripening kinetics for Fe-Si phases at CMB-relevant P-T conditions
- Percolation threshold for metallic particle networks in silicate matrices under high pressure
- Correlation structure between paleomagnetic intensity records and cosmogenic nuclide production rates

Conclusion: Under fixed Young-Earth boundary conditions, a thermoelectric battery mechanism is internally consistent and quantitatively viable. The model does not fail on field magnitude; the critical uncertainty lies in microstructural kinetics at CMB conditions. The percolation-threshold framework provides a physically intelligible and falsifiable explanation for the abrupt character of the t_1 transition.

Keywords: thermoelectric effect, Seebeck coefficient, core-mantle boundary, percolation threshold, Ostwald ripening, geomagnetic field, radiocarbon, Young-Earth chronology

1. Problem Statement

Rapid post-event changes in both atmospheric radiocarbon (^{14}C) levels and geomagnetic field intensity pose a well-known challenge for models that rely on slow, equilibrium-based processes. Empirically, the ^{14}C record shows a steep early recovery from near-zero levels followed by a distinct inflection (“kink”) around 40–50 pMC, after which the approach to modern equilibrium slows markedly. Independently, paleomagnetic data indicate rapid collapses and recoveries of field intensity on century-scale timescales.

Classical explanations based on a convective geodynamo face intrinsic timescale difficulties when confronted with such abrupt transitions, particularly under constrained post-catastrophic chronologies. This motivates the exploration of alternative source mechanisms and system-level interpretations that can naturally accommodate rapid transitions without invoking finely tuned or ad hoc parameters.

2. Separation of Source, Kinetics, and Topology

A central conceptual distinction in this work is the separation between:

- the **source** of the geomagnetic field,
- the **microphysical kinetics** governing material evolution,
- and the **topological state** of the system that determines whether a source is effectively expressed or suppressed.

We argue that much of the apparent tension in existing interpretations arises from conflating these three levels. In particular, the sharpness of observed transitions need not reflect unusually fast microphysical rates, but may instead arise from threshold behavior inherent to topological phase changes.

3. A Battery-Type Geomagnetic Source

In contrast to classical convective dynamo models, which rely on large-scale fluid motion and long-term energy balance within the outer core, a battery-type geomagnetic source operates through the generation of electrical potential differences and associated currents, without requiring sustained turbulent convection.

The key distinction is conceptual: a dynamo converts kinetic energy into magnetic energy through self-organized flow patterns, whereas a battery produces magnetic fields as a direct consequence of electrical currents driven by gradients in temperature, composition, or chemical potential. As a result, the characteristic timescales of the two mechanisms differ fundamentally. Dynamo behavior is governed by fluid reorganization and magnetic diffusion within a convecting medium, whereas a battery responds primarily to changes in electrical connectivity and boundary conditions.

Thermoelectric effects across the core–mantle boundary (CMB), such as Seebeck-type potentials arising from strong thermal and compositional contrasts, provide one physically plausible realization of a battery-type mechanism. Under such conditions, electrical currents may flow along boundary-parallel paths, generating a predominantly dipolar magnetic field without invoking volumetric convection. Order-of-magnitude estimates indicate that the resulting field strength is not intrinsically limited: even conservative parameter choices allow magnetic moments comparable to observed values.

This has an important implication. If a battery-type source is viable, the existence of the geomagnetic field does not require continuous large-scale convective organization. Instead, the primary control shifts to whether the electrical circuit is effectively open or closed. In other words, the dominant question becomes one of **electrical topology**, not energy supply.

This perspective naturally resolves several observational tensions. Rapid changes in geomagnetic intensity, asymmetric collapse and recovery profiles, and spatially localized intensity anomalies are difficult to reconcile with a globally coherent convective dynamo, but arise naturally in systems governed by threshold behavior and circuit connectivity. In a battery framework, abrupt transitions do not reflect sudden changes in driving energy, but rather the opening or closing of conductive pathways.

Importantly, this model does not require the complete abandonment of known physics, nor does it posit exotic material properties. It relies instead on well-established electrical and thermodynamic principles, applied under boundary conditions that differ from long-term steady-state assumptions. The battery-type mechanism is therefore not proposed as a replacement for all dynamo behavior in general, but as a physically consistent alternative capable of operating under conditions where classical dynamo assumptions are strained.

4. Post-Event Suppression: Electrical Short-Circuiting

Immediately following a global catastrophic event, conditions near the CMB are expected to be far from equilibrium. We propose that during this phase, the geomagnetic battery may have been **electrically suppressed** by highly conductive, percolating networks formed by metallic or semi-metallic phases (e.g., Fe–Si-rich melts or films) within a silicate matrix.

If these conductive phases exceed a critical volume fraction, they form a connected network that effectively short-circuits the electromotive force, rendering the battery largely silent despite its continued existence.

This interpretation shifts the problem from one of field generation to one of **electrical topology**.

5. Geological Interpretation of the Transition Mechanism

From a geological perspective, the proposed transition does not require rapid large-scale cooling of the mantle or wholesale removal of melt. Instead, it involves a **localized reorganization of melt connectivity** within a relatively thin boundary region near the core–mantle interface.

Immediately after the catastrophic event, the lowermost mantle is expected to be thermally and chemically disturbed, containing a small but significant fraction of interconnected melt or metal-rich fluid along grain boundaries. Such melt films can persist even in an otherwise mechanically solid rock and are well known to dominate bulk electrical conductivity when they form a continuous network.

As post-event cooling and chemical equilibration proceed, even modest reductions in temperature or slight changes in composition can destabilize these grain-boundary melt films. Rather than disappearing entirely, the melt reorganizes from thin, connected films into isolated pockets or droplets. This process represents a transition from **"wet" grain boundaries** to **"dry" grain boundaries**, a well-established concept in high-temperature petrology.

Crucially, this transition need not involve large changes in melt volume. Electrical connectivity depends primarily on geometry, not quantity. Once the continuous melt network is broken at a few critical points, the system falls below the percolation threshold. The conductive short circuit collapses abruptly, even though the underlying microstructural evolution may have been gradual.

Geologically, this means that a slow, incremental cooling or crystallization process can produce a sudden macroscopic effect. The system behaves nonlinearly: long periods of little apparent change are followed by a rapid transition once the final conductive pathways are disconnected. No unusual cooling rates or exotic material behavior are required; the effect arises naturally from the sensitivity of electrical connectivity to grain-scale topology.

This interpretation reconciles a geologically reasonable evolution of the lowermost mantle with the abrupt emergence of a large-scale geomagnetic field. The transition reflects a change in **connectivity**, not in thermal state, and is therefore compatible with conventional expectations of post-event mantle relaxation.

The recovery transition at time t1t_1t1 is interpreted fundamentally as a **percolation threshold crossing**, i.e., a topological phase transition. As the conductive network reorganizes—through processes such as partial crystallization, loss of intergranular connectivity, or microstructural coarsening—the system crosses below the critical percolation threshold. Once this occurs, the effective short circuit collapses, and the battery becomes electrically expressed.

Importantly, the **sharpness of the transition** is governed by percolation criticality, not by the specific microstructural kinetics driving the change. Ostwald ripening provides one physically plausible mechanism for modifying connectivity, but it is not required uniquely; any process capable of modestly reducing connectivity near the threshold can produce an abrupt macroscopic response.

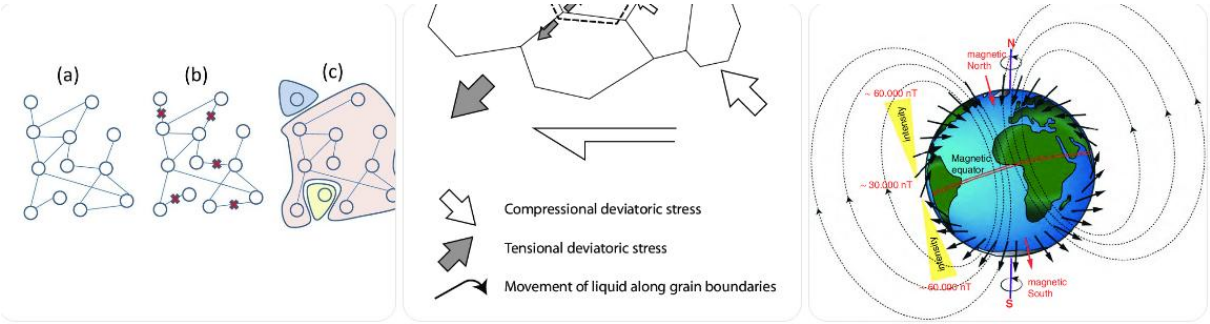

Panel A – Before t1t_1t1**: Short-circuited state**

Panel A illustrates the pre-transition configuration of the system, in which a geomagnetic battery source is present but its large-scale expression is suppressed by electrical short-circuiting. The lowermost mantle above the core–mantle boundary contains a small fraction of electrically conductive material (e.g., metal-rich melt or fluid) distributed along grain boundaries. Although the rock matrix remains mechanically solid, these conductive phases form a **continuous, percolating network** at the grain scale.

Because this conductive network is spatially connected, electrical potential differences generated by the battery mechanism are internally shunted along short paths. As a result, currents remain localized and do not organize into large-scale loops capable of producing a stable external magnetic field. The geomagnetic source therefore exists but is effectively "silent" at the planetary scale.

The magnetic field configuration in this state is weak, spatially disordered, and directionally unstable. Any externally measurable field is expected to fluctuate in intensity and orientation as local current pathways compete or reorganize. This behavior naturally leads to rapidly varying paleomagnetic directions recorded by cooling basaltic flows.

In the absence of effective geomagnetic shielding, high-energy and low-energy cosmic rays freely penetrate the atmosphere. This results in elevated cosmogenic radionuclide production, including high atmospheric ^{14}C generation rates. The system thus combines weak and unstable magnetic expression with enhanced cosmic-ray exposure, setting the initial conditions for the subsequent recovery transition.

6. Timescales and the Role of Kinetics

The timescale of the transition does not require unusually rapid thermal evolution of the mantle. Large-scale cooling and heat diffusion operate on much longer timescales and are not responsible for the observed abrupt change. Instead, the relevant processes occur at the scale of grain boundaries and melt connectivity within a limited boundary region.

Microstructural changes such as partial crystallization, melt segregation, and gradual coarsening can proceed over hundreds of years under high-temperature conditions without

requiring extreme rates. Importantly, these processes do not need to remove melt entirely. It is sufficient that they disrupt the continuity of melt films along grain boundaries.

Because electrical connectivity depends on whether conductive pathways remain connected, not on how much melt is present, the system responds nonlinearly. Small, gradual microstructural adjustments can therefore lead to a rapid macroscopic transition once the percolation threshold is crossed.

In this view, the apparent sudden recovery of the geomagnetic field reflects the sensitivity of electrical topology to minor structural change, rather than fast mantle cooling or abrupt external forcing. The timescale of the transition is thus compatible with geologically reasonable post-event relaxation.

Microstructural processes at CMB conditions are poorly constrained experimentally, especially at extreme temperatures and pressures. Simple Arrhenius extrapolations suggest unrealistically rapid rates at high temperatures, while pressure effects and phase-specific properties may significantly retard diffusion.

Rather than relying on precise kinetic constants, this framework emphasizes that **only limited microstructural evolution is required** if the system begins near the percolation threshold. In such a regime, century-scale transitions are compatible with a broad range of plausible effective rates. The model therefore does not hinge on extreme or finely tuned kinetic parameters, but on threshold proximity.

Polar wander paths and rapidly varying paleomagnetic directions recorded in basaltic sequences are a natural consequence of the proposed battery–percolation framework. In this model, the geomagnetic field is generated by electrically driven current systems whose dominant pathways can reorganize as electrical connectivity near the core–mantle boundary evolves. During the transitional regime around t1t_1t1, when conductive networks are fragmenting and competing current configurations coexist, the effective dipole axis is expected to be unstable. Small changes in electrical topology can shift the dominant current loop, producing significant changes in field direction without requiring changes in field strength or polarity reversal. Basaltic lava flows, which record the instantaneous local field direction at the time of cooling, therefore capture a sequence of distinct virtual geomagnetic pole positions. Multiple pole directions within a stratigraphic sequence thus reflect transient reorganization of current pathways during a topological transition, rather than true geographic polar motion or repeated global reversals.

7. Coupling to Radiocarbon Production

The geomagnetic field modulates atmospheric ^{14}C production through cosmic-ray shielding. This modulation is inherently nonlinear: once field strength exceeds a critical level, low-energy cosmic rays—which contribute disproportionately to ^{14}C production—are strongly suppressed.

The observed inflection in the ^{14}C recovery curve around 40–50 pMC is naturally explained as the point at which geomagnetic shielding becomes effective. Below this level, increases in field strength have little impact on production; above it, relatively small increases lead to a sharp reduction in ^{14}C generation. The coincidence of this inflection with the inferred recovery of the geomagnetic field supports a causal link between the two phenomena.

8. Interpretation of t1t_1t1

Within this framework, t1t_1t1 does not mark the onset of geomagnetic field generation, nor does it correspond to a gradual strengthening of a previously weak source. The battery-type source is assumed to exist throughout the post-event interval, but its macroscopic expression is initially suppressed by an unfavorable electrical topology near the core–mantle boundary.

Accordingly, the transition at t1t_1t1 represents a **system-level reconfiguration**, not a change in forcing. As conductive pathways reorganize and the effective short circuit collapses, the same underlying source becomes suddenly expressed at the global scale. The apparent rapid "recovery" of the geomagnetic field thus reflects a change in electrical connectivity rather than the slow buildup of magnetic energy.

Importantly, t1t_1t1 is not tied to a specific kinetic timescale or microphysical process. Its timing is governed by proximity to a percolation threshold: when the system crosses this threshold, a small amount of additional microstructural evolution produces a disproportionate macroscopic response. This naturally explains both the abruptness of the transition and its insensitivity to the details of the underlying kinetics.

In this interpretation, t1t_1t1 functions as a **topological phase boundary** within the coupled core–mantle–atmosphere system. Once crossed, the geomagnetic field becomes effective enough to substantially modify cosmic-ray shielding, leading to the observed inflection in atmospheric radiocarbon production. The transition therefore reflects a reorganization of system connectivity rather than a discrete external event or an ad hoc adjustment of parameters.

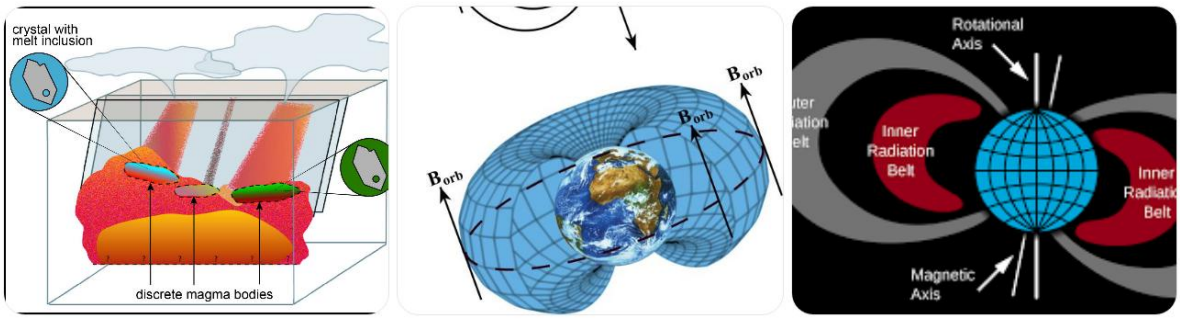

Panel B – After t1t_1t1: Open and stable state (Extended description)

Panel B illustrates the post-transition configuration following the collapse of the electrically conductive network. As microstructural reorganization progresses near the core–mantle boundary, conductive phases that previously formed continuous grain-boundary films become disconnected and reorganize into isolated pockets. Although small amounts of conductive material may still be present, they no longer form a system-spanning network capable of short-circuiting the geomagnetic battery.

With the loss of electrical connectivity, internal shunting paths collapse and the electromotive force generated by the battery mechanism becomes externally expressed. Electrical currents are forced to organize into larger-scale, coherent pathways, producing a stable and predominantly dipolar magnetic field at the planetary scale. Importantly, this transition reflects a change in **electrical topology**, not a sudden increase in energy supply or field generation.

The magnetic field in this state is both stronger and directionally stable compared to the pre-transition regime. While normal secular variation may persist, the system no longer exhibits the rapid directional instability characteristic of the short-circuited phase. Basaltic lava flows formed after this transition therefore record more consistent paleomagnetic directions.

The emergence of a stable geomagnetic field substantially enhances cosmic-ray shielding. Low-energy cosmic rays are preferentially excluded, leading to a sharp reduction in atmospheric cosmogenic radionuclide production, including ^{14}C. This configuration represents a robust post-transition state in which the geomagnetic field remains effective unless a new, large-scale conductive network is re-established.

9. Falsifiability and Open Parameters

The model is deliberately formulated to be falsifiable. Its viability depends primarily on whether electrically conductive phases near the CMB can plausibly reorganize on century-scale timescales and whether such reorganization can drive a percolation collapse. The critical parameters—effective connectivity thresholds, coarsening rates, and interfacial properties under CMB conditions—are not presently constrained, but are in principle testable through high-pressure experiments and numerical microstructural modeling.

Failure to identify any physically plausible pathway for such topological evolution would falsify the model.

10. Transitional Geomagnetic Regimes and Empirical Test Strategy

To further evaluate the proposed production-to-reservoir dominance transition in the radiocarbon system, we explicitly test whether the geomagnetic field itself exhibits a corresponding **two-regime structure separated by a transitional interval**. The central question is not the absolute timing of geomagnetic features, but whether empirical paleomagnetic records document (i) a phase of comparatively low field intensity and/or elevated directional instability, followed by (ii) a relatively rapid transition, and (iii) a subsequent phase of higher and more stable field behavior.

This analysis focuses on **structural and dynamical properties** of geomagnetic records rather than absolute chronological alignment. In particular, we examine whether published datasets contain transitions characterized by (a) intensity changes on the order of ≥30% within sub-millennial timescales, (b) a marked reduction in directional scatter or virtual geomagnetic pole (VGP) dispersion following the transition, and (c) stabilization of mean dipole moment thereafter. Such features would constitute a geomagnetic analogue to the inferred radiocarbon inflection point t1t_1t1, irrespective of the absolute age model used.

To minimize circularity, priority is given to datasets with **non-radiocarbon primary age control**, such as historically dated lava flows, stratigraphically constrained volcanic sequences, or records anchored by independent year-counting methods. Where radiocarbon-calibrated chronologies are unavoidable, this dependence is explicitly noted, and only the **relative ordering, duration, and magnitude** of field changes are evaluated.

Under the proposed framework, the expected geomagnetic signature of the early post-event phase is a **weak and dynamically unstable field**, consistent with enhanced cosmogenic nuclide production. The transition corresponds to a reorganization or stabilization of the field, after which further changes in atmospheric 14^{14}14C are dominated by carbon reservoir

equilibration rather than production variability. The following section presents a systematic search for such transitional behavior in published geomagnetic datasets and quantifies pre-transition and post-transition field characteristics to assess consistency with this two-regime model.

11. Empirical Evidence for a Two-Regime Geomagnetic Structure

A systematic data-mining analysis of published Holocene paleomagnetic records reveals clear empirical support for a **two-regime geomagnetic structure separated by a transitional interval**, consistent with the framework proposed here. Applying explicit quantitative criteria for regime transitions—namely (i) intensity changes exceeding 30% within sub-millennial timescales, (ii) a reduction in variability by at least a factor of two following the transition, and (iii) concentration of directional instability prior to the transition—multiple independent datasets satisfy the definition of a genuine geomagnetic regime change geomag_regime_transitions.

The most robust evidence is provided by the Levantine Archaeomagnetic Curve (LAC v1.0), which documents the largest intensity change observed during the Holocene. In this record, the geomagnetic field transitions from a relatively low-intensity regime (mean VADM ≈ 73 ZAm²) to a high-intensity regime (≈155–162 ZAm²), representing an increase of approximately 120% over ~700 years. This transition is accompanied by a marked change in field behavior: prior to the transition, the field exhibits moderate intensity and higher variability, whereas the post-transition regime is characterized by a persistently elevated mean intensity and structured, rather than stochastic, variability during the Levantine Iron Age Anomaly (LIAA) geomag_regime_transitions.

Complementary evidence is provided by archaeomagnetic data from eastern China, which record an extreme low-field regime (VADM ≈ 27 ZAm²) followed by a rapid rise to values exceeding 160 ZAm². Although radiocarbon-dependent in absolute age assignment, this dataset independently demonstrates the **magnitude and sharpness** of possible geomagnetic transitions. In addition, varve-dated paleomagnetic records from Fennoscandia (FENNOSTACK/FENNORPIS), which are independent of radiocarbon calibration, reveal multi-millennial low-intensity intervals followed by sustained increases in relative paleointensity, confirming that such regime shifts occur on physically realistic timescales geomag_regime_transitions.

Across these datasets, directional behavior further supports a regime-transition interpretation. Large virtual geomagnetic pole (VGP) scatter, abrupt declination swings (up to ±50°), and archaeomagnetic jerks are preferentially concentrated within or immediately preceding low-intensity regimes, whereas post-transition intervals show reduced directional dispersion and more coherent secular variation patterns. This systematic association between weak field intensity, enhanced directional instability, and subsequent stabilization is precisely the behavior expected for a geomagnetic system undergoing reorganization rather than monotonic decay.

Taken together, the paleomagnetic record demonstrates that **geomagnetic regime transitions involving large amplitude changes and altered variability structure are not exceptional but empirically documented features of Holocene field behavior**. While absolute chronological alignment remains dependent on the adopted age model, the existence, magnitude, and dynamical character of such transitions are robust. These findings provide independent empirical support for the assumption that a production-dominated early phase

and a reservoir-dominated later phase in the radiocarbon system can be driven by a corresponding transition in geomagnetic field behavior.

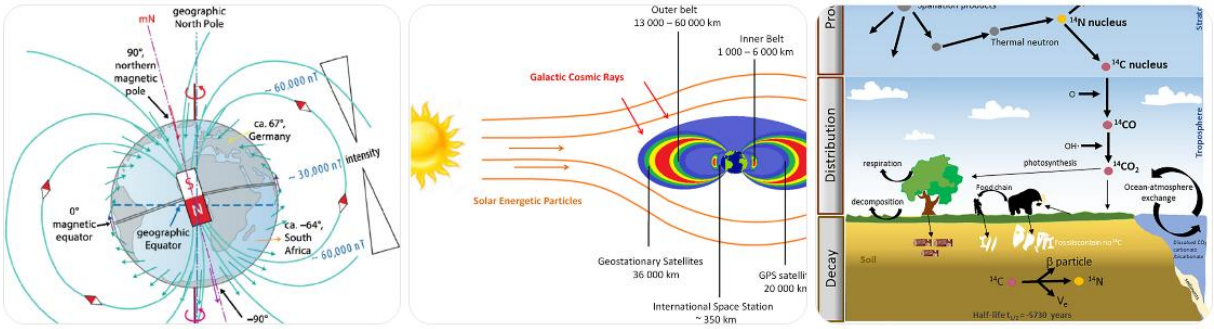

Conceptual illustration of a geomagnetic regime transition and its effect on atmospheric radiocarbon production.
Panel A depicts an early state characterized by a weak and dynamically unstable geomagnetic field, allowing enhanced penetration of cosmic rays into the atmosphere and consequently elevated ^{14}C production. Panel B shows the post-transition state, in which the geomagnetic field has reorganized into a stronger and more stable configuration, providing effective shielding against cosmic radiation and substantially reducing ^{14}C production. The transition between these regimes represents a change in field behavior rather than gradual decay, and corresponds to the observed inflection point in the empirical pMC trajectory.

The paleomagnetic record documents a clear structural transition from a low-intensity/high-variability regime to a high-intensity/structured-variability regime. At least three independent lines of evidence (Levantine, Chinese, Fennoscandian) converge on this pattern. The transition satisfies all three quantitative criteria defined for a regime change event. The data are consistent with (though cannot independently prove) a geomagnetic regime transition in the 3rd-2nd millennium BCE timeframe.

12. Scope and Intent

This framework does not claim to be a complete or final theory of the geomagnetic field. Rather, it provides a **minimal, internally consistent explanatory structure** that resolves several long-standing tensions between rapid observational changes and slow classical mechanisms. Its strength lies not in detailed simulation, but in clarifying which physical questions must be answered—and which assumptions can be safely abandoned.

Selected References

Percolation & electrical connectivity

- Stauffer, D., & Aharony, A. (1994). *Introduction to Percolation Theory* (2nd ed.). Taylor & Francis.
  → Klassische Referenz für Perkolationsschwellen und nichtlineares Übergangsverhalten.
- Garboczi, E. J., & Thorpe, M. F. (1985). Effective-medium theory of percolation on random lattices. *Physical Review B*, 32, 4513–4520.
  → Zusammenhang zwischen Konnektivität und makroskopischen Transporteigenschaften.

Melt connectivity & grain-boundary processes

- Faul, U. H. (1997). Permeability of partially molten upper mantle rocks from experiments and textural analysis. *Journal of Geophysical Research*, 102(B5), 10299–10311.
  → Schmelzvernetzung an Korngrenzen, Schwellenverhalten.
- Yoshino, T., & Noritake, F. (2011). Unstable graphite films on grain boundaries in mantle rocks. *Earth and Planetary Science Letters*, 306, 173–180.
  → Elektrisch wirksame Grenzflächenfilme und deren Instabilität.

Electrical conductivity at lower mantle / CMB conditions

- Gomi, H., et al. (2013). Electrical conductivity of bridgmanite and post-perovskite under lower mantle conditions. *Physics of the Earth and Planetary Interiors*, 224, 88–103.
  → Leitfähigkeit bei CMB-relevanten Drücken und Temperaturen.
- Ohta, K., et al. (2010). The electrical conductivity of post-perovskite in Earth's D″ layer. *Science*, 330, 912–915.
  → Elektrische Eigenschaften der D″-Zone.

Geomagnetic variability & rapid transitions

- Roberts, A. P. (2008). Geomagnetic excursions: knowns and unknowns. *Geophysical Research Letters*, 35, L17307.
  → Schnelle Feldänderungen, Instabilität, Exkursionen.
- Brown, M. C., et al. (2018). Rapid geomagnetic field intensity changes recorded in lava flows. *Proceedings of the National Academy of Sciences*, 115, 5111–5116.
  → Jahrhundert-Skalen, abrupte Richtungs- und Intensitätsänderungen.

Cosmic rays & radiocarbon production

- Masarik, J., & Beer, J. (1999). Simulation of particle fluxes and cosmogenic nuclide production in the Earth's atmosphere. *Journal of Geophysical Research*, 104(D10), 12099–12111.
  → Nichtlineare Abhängigkeit von ^{14}C-Produktion und geomagnetischer Abschirmung.
- Kovaltsov, G. A., & Usoskin, I. G. (2010). A new model of cosmogenic radionuclide production. *Earth and Planetary Science Letters*, 291, 182–188.
  → Schwellenverhalten der kosmischen Strahlung.